JOURNAL OF NEUROPHYSIOLOGY
Vol. 66, No. 6, December 1991. *Printed in U.S.A.*

Discharge Characteristics of Medial Rectus and Abducens Motoneurons in the Goldfish

ANGEL M. PASTOR, BLAS TORRES, JOSÉ M. DELGADO-GARCIA, AND ROBERT BAKER
Laboratorio de Neurociencia, Departamento de Fisiología y Biología Animal, Facultad de Biología, Universidad de Sevilla, 41012 Seville, Spain; and Department of Physiology and Biophysics, New York University Medical Center, New York, New York 10016

SUMMARY AND CONCLUSIONS

1. The discharge of antidromically identified medial rectus and abducens motoneurons was recorded in restrained unanesthesized goldfish during spontaneous eye movements and in response to vestibular and optokinetic stimulation.

2. All medial rectus and abducens motoneurons exhibited a similar discharge pattern. A burst of spikes accompanied spontaneous saccades and fast phases during vestibular and optokinetic nystagmus in the ON-direction. Firing rate decreased for the same eye movements in the OFF-direction. All units showed a steady firing rate proportional to eye position beyond their recruitment threshold.

3. Motoneuronal position (k_s) and velocity (r_s) sensitivity for spontaneous eye movements were calculated from the slope of the rate-position and rate-velocity linear regression lines, respectively. The averaged k_s and r_s values of medial rectus motoneurons were higher than those of abducens motoneurons. The differences in motoneuronal sensitivity coupled with structural variations in the lateral versus the medial rectus muscle suggest that symmetric nasal and temporal eye movements are preserved by different motor unit composition. Although the abducens nucleus consists of distinct rostral and caudal subgroups, mean k_s and r_s values were not significantly different between the two populations.

4. Every abducens and medial rectus motoneuron fired an intense burst of spikes during its corresponding temporal or nasal activation phase of the "eye blink." This eye movement consisted of a sequential, rather than a synergic, contraction of both vertical and horizontal extraocular muscles. The eye blink could act neither as a protective reflex nor as a goal-directed eye movement because it could not be evoked in response to sensory stimuli. We propose a role for the blink in recentering eye position.

5. Motoneuronal firing rate after ON-directed saccades decreased exponentially before reaching the sustained discharge proportional to the new eye position. Time constants of the exponential decay ranged from 50 to 300 ms. Longer time constants after the saccade were associated with backward drifts of eye position and shorter time constants with onward drifts. These postsaccadic slide signals are suggested to encode the transition of eye position to the new steady level.

6. Motoneurons modulated sinusoidally in response to sinusoidal head rotation in the dark, but for a part of the cycle they went into cutoff, dependent on their eye position recruitment threshold. Eye position (k_v) and velocity (r_v) sensitivity during vestibular stimulation were measured at frequencies between $^1/_{16}$ and 2 Hz. Motoneuronal time constants ($\tau_v = r_v/k_v$) decreased on the average by 25% with the frequency of vestibular stimulation. The decrease was largely explained by an increase in the k_v coefficient with frequency. Variation of the firing-related parameters with the frequency of sinusoidal head rotation and the presence of postsaccadic slide demonstrate that the behavior of goldfish extraocular motoneurons deviates from the predictions of a first-order model.

7. Bode plots obtained from either the phase shift between firing rate and eye position or from the motoneuronal time constant (τ_v) at each tested frequency were less steep than those calculated from a single time constant approximation ($\tau_s = r_s/k_s$). Linearization of Bode plots showed that at least two slopes described motoneuronal response with higher accuracy. This result indicates that motoneuronal discharge characteristics would be fit better by higher-order linear approximations, as has been previously described for mammalian extraocular motoneurons.

8. An anatomic basis for a recruitment order dictated by motoneuronal size was examined after horseradish peroxidase and biocytin injection into the lateral and medial rectus muscles. Soma sizes were uniformly distributed over a twofold range and showed no preference for location according to size; however, abducens motoneurons often formed small clusters of three to six somas of similar size. Dendrites of medial rectus motoneurons extended toward and around the medial longitudinal fasciculus. The dendrites of both subgroups of abducens nucleus motoneurons were oriented toward the same areas (largely lateral) in the caudal brain stem. Comparison of the results obtained with the two staining techniques revealed biocytin to be more useful because complete dendritic and axonal organization could be visualized.

9. Recruitment pattern within medial rectus and abducens motoneuron populations was related to several functional parameters, especially k_s and r_v. Motoneurons with higher thresholds tended to exhibit higher k_s and r_v values. Significant inverse linear relationships were found between antidromic latency, as a likely indicator of cell size, and k_s values. Linear relationships between antidromic latency and unit threshold were not significant. These findings indicate that, within both motoneuronal groups, a recruitment order is established in accordance with certain firing-related parameters. However, structural variation alone cannot sufficiently explain recruitment.

INTRODUCTION

The basic extraocular muscle reference frames and the organization of motor nuclei are well conserved from teleosts through mammals. The six extraocular muscles that rotate the eye are innervated by four ipsilateral (medial rectus, inferior rectus, inferior oblique, and lateral rectus) and two contralateral (superior rectus and superior oblique) motoneuronal pools (Allum et al. 1981; Easter 1979; Graf and Baker 1985; Graf and McGurk 1985; Hadidian and Dunn 1938; Luiten and Dijkstra-De Vlieger 1978; Sterling 1977; Szabo et al. 1987). One of the most interesting features in teleostean oculomotor organization is that the abducens nucleus is divided into two subnuclei, both of which innervate the lateral rectus muscle. This arrangement, unique among vertebrates, offers a model to test whether anatomi-

cally separate subgroups of abducens motoneurons could also be functionally distinct (Gestrin and Sterling 1977). Indeed, considerable attention has been devoted to the basic question of distinguishing whether motoneurons innervating extraocular muscles can be grouped into either a single category and/or multiple categories according to their qualitative discharge characteristics (De la Cruz et al. 1989; Delgado-García et al. 1986a; Dieringer and Precht 1986; Fuchs and Luschei 1970; Fuchs et al. 1988; Gestrin and Sterling 1977; Henn and Cohen 1972; Robinson 1970). Nonetheless, controversy still reigns regarding the observations obtained in different species. For instance, the report on unidentified goldfish abducens motoneurons suggested a separation of function between the two subdivisions of the abducens nucleus that would match the two basic fiber types found in the extraocular muscles of this teleost (Gestrin and Sterling 1977). A similar functional segregation of identified abducens motoneurons was observed to reflect the contractile properties of three muscle fiber types in frogs (Dieringer and Precht 1986). By contrast, cat and monkey abducens motoneurons could not be divided into functional subgroups because all the motoneurons participated in the basic tonic-phasic discharge pattern (Delgado-García et al. 1986a; Fuchs and Luschei 1970; however, see Henn and Cohen 1972). In addition, the described discharge properties of medial rectus motoneurons, in both fish and mammals, did not support the separate processing of eye position and velocity signals (De la Cruz et al. 1989; Hermann 1971; Korn and Bennett 1975; Robinson 1970). Thus the present work was carried out to characterize the discharge pattern of antidromically identified motoneurons mediating eye movements about the vertical axis to further investigate the functional significance of a rostral and caudal population of abducens motoneurons.

In addition to the qualitative profile of discharge, a second aspect of muscle force regulation is the extent to which an individual motoneuron participates in the production of a certain eye position or fixation. Recruitment threshold, motoneuronal eye position, and velocity sensitivity are not fixed values within a pool of motoneurons. A number of studies have reported that some of these properties are graded to produce a recruitment pattern (Delgado-García et al. 1986a; Fuchs and Luschei 1970; Fuchs et al. 1988; Gestrin and Sterling 1977; Robinson 1970; Skavensky and Robinson 1973). Two likely interacting mechanisms could produce such a recruitment pattern: namely, either an order within premotor afferents to motoneuronal pools (Delgado-García et al. 1986b; Iwamoto et al. 1990) or the passive and/or active electrophysiological properties of the motoneuron (Cullheim 1978; Grantyn and Grantyn 1978; Henneman et al. 1965). In the present report, the possible contribution of each mechanism to a recruitment order was investigated by correlating functional parameters with indirect morphological features such as axonal conduction velocity.

Finally, the qualitative and quantitative firing properties of abducens versus medial rectus motoneurons were compared during the repertoire of horizontal eye movements. This evaluation was carried out in view of the anatomic differences concerning size, fiber number, and type composition reported between the medial rectus and the lateral rectus muscles in teleosts (Davey et al. 1975; Easter 1979; Graf and McGurk 1985; Kumari et al. 1979). Because morphological differences are likely reflected at the functional level, medial rectus and abducens motoneurons discharge characteristics were analyzed to gain insight into how premotor and motor elements process information to produce appropriate versional eye movements. Part of this work has been presented in abstract form (Pastor and Baker 1989; Pastor et al. 1989).

METHODS

Animals

Single-unit and field potential recordings were carried out in 12 goldfish (*Carassius auratus*), 20 cm long from snout to tail base, obtained from authorized suppliers (Hunting Creek Fisheries, Thurmont, MD). Goldfish were maintained in aquaria at 20°C for ≥2 wk before any experiment. In another 12 goldfish, individual extraocular muscles were injected with either horseradish peroxidase (HRP) or biocytin for morphometric measurements of motoneuron structure.

Preexperimental surgical preparation

As a standard procedure, each fish was anesthetized with tricaine methasulfonate (1:20,000 wt/vol). The fish was clamped between two sponge-plastic pads in a Plexiglas tank. The tapered end of a plastic tube connected to a motor-propelled water circuit was carefully fitted to the mouth to ensure a constant flow through the gills. Water was continuously aerated and kept at 20°C with a Peltier-effect heat exchanger. The water flow was set at 200 ml/min, which is sufficient to avoid active ventilatory movements in an unanesthetized goldfish. To ensure head stability during recording, a dental acrylic platform fastened to the frontal bones was connected to the tank during the experiments. Animals prepared for either abducens or oculomotor nucleus recordings were chronically implanted with appropriate antidromic bipolar stimulating electrodes through a 2 × 2-mm window opened in the overlying frontal bones. Meningeal tissues over the telencephalic lobes were gently displaced and the electrode position adjusted to produce the appropriate horizontal eye movement following a 0.05-ms single square pulse of 25 μA. The oculomotor nerve was stimulated near its exit from the brain case. The elicited eye twitch was nasally directed, with little sign of either vertical or torsional components. The electrode aimed at the abducens nerve was inserted through the optic foramen into the posterior myodome, where both lateral rectus muscles course in parallel before diverging toward their scleral insertion on each eye. To record single units from the abducens nucleus, a second window was opened in the supraoccipital bone caudal to the location of the corpus cerebelli. Recording windows were reattached with cyanoacrylic glue with the use of the piece of bone removed during surgery. Animals were allowed to recover from surgery for ≥48 h before experimental sessions started.

Eye movements and single-unit recording

At the beginning of each recording session, the fish was placed within the circular tank with its longitudinal body axis in the horizontal plane. The subtended angle of vision in the center of the tank was ±150 and ±30° in the horizontal and vertical planes, respectively. Eye movements were recorded with the use of the scleral search coil technique. An 80-turn coil made of enamel-insulated 25-μm copper wire, 2.3-mm OD, was sutured to the upper scleral margin of each eye. Lidocaine solution (4%) was adminis-

tered topically to the sclera before the eye coil was attached. The tank was placed within the magnetic field so that the eyes were in the center. Eye movement calibration was obtained by rotating the magnetic field coils at known angles around the stationary eye coils. Zero eye position in the orbit was defined as the middle of the eye movement range after 15 min of spontaneous eye movements.

Single-unit and field potentials were recorded with glass microelectrodes filled with 2.5 M NaCl. Electrode resistance ranged from 1 to 5 MΩ as measured with square current pulses. Electrical activity was amplified by a high-impedance head-stage amplifier close to the preparation and then filtered at a bandwidth of 10 Hz–10 kHz. The microelectrode was controlled with a three-axis micromanipulator that minimally interfered with the fish's visual field. Electrode tracks in the oculomotor complex passed through the tectal commisure, the valvula of the cerebellum, and the ventricle before reaching the mesencephalic tegmentum (Fig. 1*A, left*). For recording in the abducens nucleus, the tela chorioidea overlying the fourth ventricle was removed to expose the medulla and tracks passed through the cerebellar crest toward the ventral aspect of the medulla (Fig. 1*A, right*). The microelectrode was angled at 20° to reach the two subdivisions of the abducens nucleus.

Vestibular and optokinetic stimulation

Sinusoidal vestibular stimulation was achieved by means of a servo-controlled turntable. Vestibular stimulation about the vertical axis was carried out in the dark at frequencies spaced in octave intervals from 1/16 to 4 Hz, including the intermediate frequencies of 1.5 and 3 Hz. Zero-to-peak head velocity was maintained constant at 16°/s over the frequency range. Optokinetic stimulation was achieved by the use of a planetarium that projected a random pattern of light spots, each subtending 3° on the wall of the circular tank. The planetarium was sinusoidally driven around the vertical axis by a servo-controlled motor at frequencies ranging from 1/16 to 1/4 Hz and at 16°/s zero-to-peak velocity. The servo-controlled vestibular rate table and planetarium were interfaced by a digital function generator, allowing for any interaction in gain (the ratio of planetarium velocity to table velocity) and/or phase between both stimuli.

Data storage and analysis

Head position, planetarium velocity, horizontal eye position, and neuronal activity were stored digitally on a custom-made video system at a sampling rate of 11 kHz for off-line analysis. Unfiltered records of antidromic activations and field potentials were either photographed directly from the cathode ray tube screen or printed on an *X-Y* plotter for latency measurements. Action potentials were fed into a window discriminator; and the Schmidt pulses, together with eye position, table position, and planetarium velocity, were digitized and stored in the computer for analysis. Computer programs were developed to display the instantaneous firing frequency (i.e., the reciprocal of the interspike intervals) of the neuronal discharge and the eye position and velocity. Data selection was carried out by cursors on the computer screen. Firing frequency was correlated to eye position and velocity during spontaneous and either visually or vestibularly induced eye movements.

Rate-position relationships for spontaneous eye movements were calculated by linear regression analysis for different intersaccadic periods through the oculomotor discharge range of the motoneuron. Rate-velocity relationships for spontaneous saccades were obtained by linear regression of the instantaneous firing rate minus the eye position component versus the eye velocity signal. Position and velocity sensitivity for eye movements induced during either vestibular or optokinetic stimulation were computed by linear multivariate regression analysis. Bode plots of phase shift between firing rate and eye position were obtained on the computer screen by scaling and manually *x*-offsetting the eye position trace to obtain the best fit in segments free of fast phases.

Histology

To study the medial rectus subdivision in the oculomotor nucleus and both subgroups of abducens motoneurons, 0.5 μl of a 30% HRP or 3% biocytin saline solution were pressure-injected into either the medial or the lateral rectus muscle. After intracardiac perfusion with teleost saline and aldehyde fixative (1% paraformaldehyde and 1.25% glutaraldehyde), 50-μm sections of the brain stem were processed with the use of the avidin-biotin-peroxidase complex (Horikawa and Armstrong 1988) for biocytin-injected animals. Both HRP and biocytin retrogradely filled motoneurons were revealed with diaminobenzidine histochemistry (Mesulam 1982). Sections were mounted onto gelatin-coated slides; air dried; and, in some instances, counterstained with cresyl violet.

RESULTS

Identification of motoneurons in the oculomotor and abducens nuclei

The oculomotor nucleus was located in the mesencephalon, lying beneath the cerebral aqueduct and close to the midline. In a parasagittal section of Nissl-stained material, it appeared as a cell column that extended rostrocaudally from 350 to 400 μm. Coronal sections of the oculomotor nucleus showed a c-like shape that surrounded the dorsomedial aspect of the medial longitudinal fasciculus (Fig. 1*A*). After either biocytin or HRP injection into the medial rectus muscle, motoneurons were located in the central aspect of the nucleus. The dendrites of medial rectus motoneurons profusely extended laterally toward and around the medial longitudinal fasciculus (Fig. 1*B*). The mean number of labeled medial rectus motoneurons was 41 ± 7 (SD). The mean averaged soma diameter was 24 ± 5 μm. Soma sizes were distributed rather uniformly over a broad range (15–38 μm). An example of the profound differences encountered in somatic size is illustrated in Fig. 1*C*.

The abducens nucleus consisted of a rostral and a caudal subdivision situated close to the ventral surface of the medulla and separated by 550–600 μm in the rostrocaudal direction. Each subdivision exhibited a spherical appearance, with tightly packaged cell bodies extending their dendritic trees radially, but preferentially, toward the medial reticular formation, the vestibular nuclei, and the caudal medulla (Fig. 1, *A, D,* and *E*). Both abducens subnuclei were found to be morphometrically identical. The mean number of labeled motoneurons after tracer injection into the lateral rectus muscle was 63 ± 6; and the mean averaged diameter was 22 ± 7 μm, with a range of 17–39 μm. Although in both nuclei (medial rectus and abducens) motoneuronal size was evenly distributed, no evidence was found for any location versus size dependence. However, motoneurons in the abducens nucleus often formed small clusters of three to six neurons of similar size (Fig. 1, *D* and *E*).

Antidromic field potentials elicited by electrical stimulation of either the IIIrd or the VIth nerve were systematically

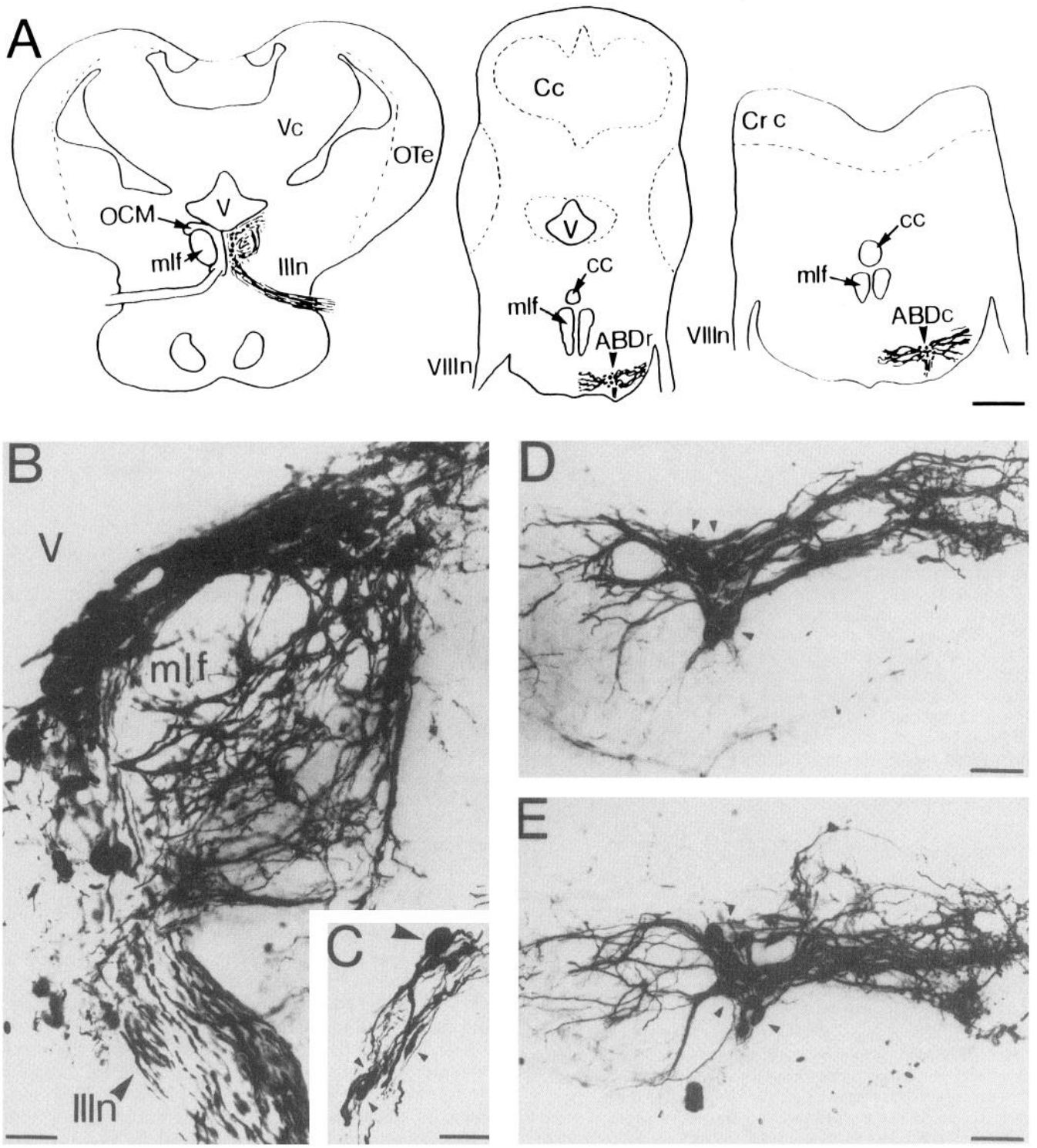

FIG. 1. Distribution of extraocular motoneurons in the goldfish retrogradely labeled with biocytin. *A*: camera lucida drawings of coronal sections through the brain stem, showing the location of the medial rectus population in oculomotor complex (OCM) and rostral (ABDr) and caudal (ABDc) subdivisions of the abducens nucleus. *B*: coronal section through the oculomotor nucleus at the level of the medial rectus, showing labeled motoneurons located around the medial longitudinal fasciculus (mlf) and underneath the ventricle (V). Note that dendrites profusely extend toward and around the ipsilateral mlf. Axons exit the nucleus in a single fascicle as a part of the oculomotor nerve (IIIn). *C*: microphotograph of medial rectus motoneurons, illustrating the difference in size between a large spherical soma and 3 small fusiform motoneurons (large and small arrowheads, respectively). *D* and *E*: coronal sections from the same brain stem, illustrating the cytoarchitecture of rostral (*D*) and caudal (*E*) subdivisions of the abducens nucleus. Arrowheads point to clusters of 3–6 somatas of nearly equal size. Calibrations are 400 μm for *A*, 40 μm for *B*, and 100 μm for *C–E*. Other abbreviations are cc, central canal; Cc, Crc, and Vc, corpus, crista, and valvula cerebelli, respectively; OTe, Optic tectum; VIIIn, octavus nerve.

used to locate their respective nuclei. A triphasic (positive-negative-positive) waveform with a maximum negative peak amplitude of ~1.5 mV was found in the center of each of these populations (not illustrated). Latencies to the maximum peak negativity were similar for the three recording sites: 1.1 ms for the oculomotor nucleus, 1 ms for the rostral and caudal subdivisions of the abducens nucleus.

Motoneurons were identified following antidromic activation from their respective cranial nerves and by the systematic use of the collision test to establish that the recorded neuron was the same as that activated (Fig. 3, *C–E*). This method was sufficient for identifying abducens motoneurons in either the rostral or caudal subdivision, but additional criteria were required for medial rectus motoneurons. Antidromically activated motoneurons in the oculomotor nucleus either discharged in close relation to horizontal eye movements or were silent except for "blinks" (see DISCHARGE ASSOCIATED WITH BLINKS.) Experiments with electrodes inserted into the medial rectus muscle and the IIIrd nerve confirmed that medial rectus motoneurons were the only subgroup in the oculomotor nucleus to show spontaneous discharge in the head-restrained condition. Identification of motoneurons with electrodes implanted in the orbit was not routinely pursued because this procedure disrupted eye movement mechanics.

Rostral and caudal abducens motoneurons were distinguished after establishing the coordinates for the two subdivisions. Latencies to the negative peak of the antidromic spikes were similar for medial rectus (0.89 ± 0.17 ms) and both abducens nucleus populations (0.93 ± 0.16 ms for rostral and 0.94 ± 0.18 ms for caudal abducens motoneurons; see Table 1). The distance from the stimulation point to the recording site was 8 mm for both nuclei. To calculate axonal conduction velocity, the latency to the first apparent positive peak was measured; a 0.2-ms utilization time subtracted and divided by the distance to the stimulating electrode. Conduction velocity was similar for medial rectus (32.4 ± 13.2 m/s), rostral abducens (30.5 ± 14.3 m/s), and caudal abducens (28.7 ± 14.5 m/s) motoneurons (Table 1).

TABLE 1. *Comparison of discharge characteristics of identified horizontal extraocular motoneurons obtained during spontaneous eye movements*

Parameter	Source of Motoneurons		
	Medial rectus	Rostral abducens	Caudal abducens
Antidromic latency, (ms)	0.89 ± 0.17	0.93 ± 0.16	0.94 ± 0.18
Conduction velocity, (m/s)	32.4 ± 13.2	30.5 ± 14.3	28.7 ± 14.5
Position gain during intersaccadic periods (k_s), spikes·s^{-1}·deg^{-1}	8.37 ± 1.71	7.13 ± 3.40	6.32 ± 1.40
Y-intercept (F_0), spikes/s	−13.68	−14.25	+10.87
Threshold, deg	1.09 ± 5.81	−0.3 ± 6.1	−2.8 ± 5.23
Velocity gain during spontaneous saccades (r_s), spike·s^{-1}·deg^{-1}	1.19 ± 0.43	0.96 ± 0.44	1.03 ± 0.37

Values are means ± SD, except for those in the *Y*-intercept row; *n* is number of motoneurons, as follows: medial rectus, 19; rostral abducens, 12; and caudal abducens, 10.

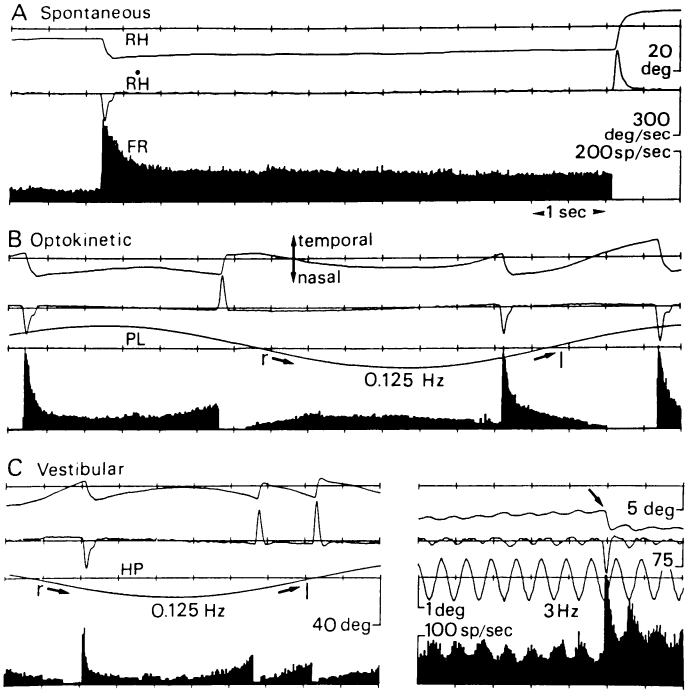

FIG. 2. Discharge of an antidromically identified medial rectus motoneuron during spontaneous eye movements and during sinusoidal optokinetic and vestibular stimulation. *A*: instantaneous firing rate (FR) during a long intersaccadic interval. *B*: discharge during optokinetic nystagmus induced by sinusoidal rotation at 0.125 Hz of the visual world projected by a planetarium (PL). *C*: responses at 0.125 and 3 Hz of sinusoidal table rotation (HP, head position). Arrow in *right panel* corresponds to a spontaneous saccade. RH and RH are right horizontal eye position and velocity, respectively. r and l indicate right and left, respectively.

Behavior during spontaneous eye movements

Spontaneous eye movements in the restrained goldfish consisted of a stereotyped pattern of saccades and intersaccadic intervals that scanned, back and forth, a field of 33 ± 2° in the horizontal plane. Qualitatively, all the medial rectus and abducens motoneurons recorded during spontaneous eye movements discharged in a tonic-phasic manner (Figs. 2*A* and 3, *A* and *B*). Firing frequency increased monotonically as the eye was held at more eccentric positions in the ON-direction. Motoneurons also exhibited a burst of spikes during ON-directed saccades and a pause during those in the OFF-direction.

FIRING RATE AND EYE POSITION RELATIONSHIPS. Eye position sensitivity during spontaneous eye movements (k_s) was calculated as the slope of the regression line between instantaneous firing frequency and eye position during intersaccadic intervals. Measurements were scattered as widely as possible throughout the whole oculomotor range. Sample size for a given intersaccadic period was optimized for the range of firing frequency observed in the recorded motoneurons (10–200 spikes/s) in steps of 50 spikes/s to account for the variability observed in the interspike intervals. Time windows for data selection varied between 400 (for frequencies <50 spikes/s) and 200 ms (for frequencies >150 spikes/s). Data were collected 500 ms after the preceding saccade

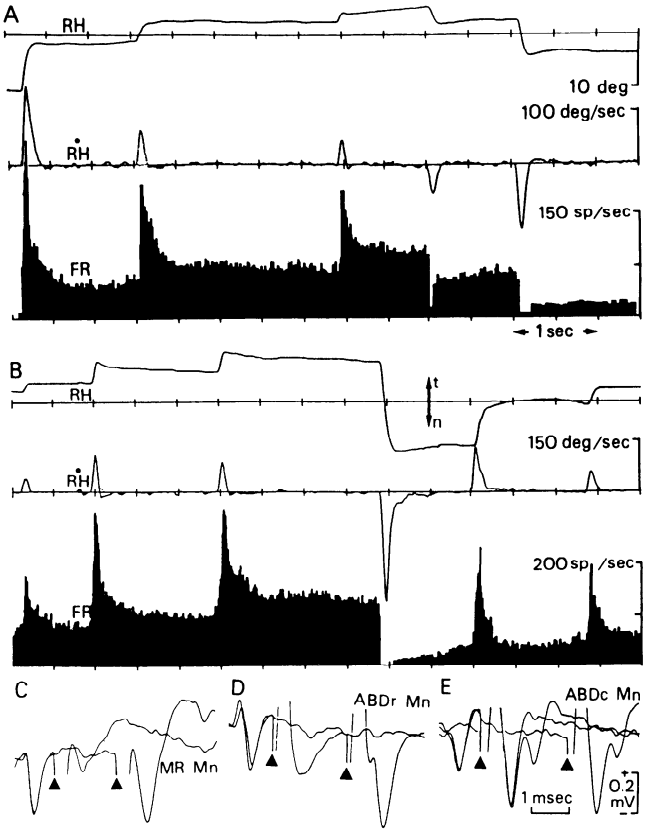

FIG. 3. Discharge characteristics of 2 typical abducens motoneurons recorded in rostral (*A*) and caudal (*B*) subdivisions of the abducens nucleus during spontaneous eye movements. Both motoneurons discharged a burst of spikes for temporal (t) saccades, paused for nasal (n) saccades, and exhibited a steady discharge that increased with more temporal eye positions. Other abbreviations as in Fig. 2. *C–E*: collision tests for a medial rectus (MR) and rostral (ABDr) and caudal (ABDc) abducens motoneurons (Mn). Triangles indicate onset of the stimulus artifact. Calibrations for *C–E* are shown in *E*.

to avoid the postsaccadic slide in firing frequency. Thus eye position sensitivity was calculated in stationary conditions on the basis of the observed time constants for the postsaccadic slide (see below). Figure 4, *A–C*, shows the lines of best fit for the rate-position relationship obtained for each motoneuronal group. The correlation coefficients (r) were always >0.8.

Mean eye position sensitivity was 8.37 ± 1.71 spikes·s^{-1}·deg^{-1} for medial rectus (n = 19), 7.13 ± 3.4 spikes·s^{-1}·deg^{-1} for rostral abducens (n = 12), and 6.32 ± 1.4 spikes·s^{-1}·deg^{-1} for caudal abducens motoneurons (n = 10) (Table 1). When these mean k_s values were compared, no significant differences ($P > 0.2$) were found between the two abducens nucleus populations. Conversely, eye position sensitivity was slightly larger ($P < 0.05$) for medial rectus than for abducens motoneurons considered as a single population.

The eye position threshold at which each motoneuron was recruited into activity was estimated by extrapolation of the line that best fit the rate-position data. An attempt was made to obtain a real behavioral threshold for several units as the turntable was slowly rotated by hand and then left stationary. Firing frequency of every motoneuron tested in this way abruptly jumped from zero to 8–15 spikes/s. This observation suggested that calculated thresholds were slightly shifted toward the OFF-direction. Mean threshold centered around 0° for the three motoneuronal groups (Table 1). The Y-axis intercept (F_0, spikes/s) represents the firing rate at the midposition of the eye in the orbit. Because about one-half of the recorded neurons were silent at this eye position, either negative or very low values were obtained for mean F_0 (Table 1). If only the positive F_0 values are taken into consideration, then similar mean F_0 values of ~30 spikes/s were obtained for the three motoneuronal groups ($P > 0.2$).

Regularity of firing rate was assessed by calculating the coefficient of variation determined as the percentage ratio of the standard deviation to the mean instantaneous firing rate. The measurement was performed at a number of different eye positions for each motoneuron. The average coefficient of variation at frequencies >30 spikes/s ranged between 5 and 17% for both medial rectus and abducens motoneurons. The coefficient of variation was fairly constant through the firing frequency range for all the units but was 20–40% higher when mean firing rates were <25–30 spikes/s (Fig. 5*A*). Regularity of firing was also studied as a function of time for intersaccadic intervals up to 5 s, with mean frequencies between 90 and 150 spikes/s. Despite small fluctuations, the coefficient of variation did not show any trend over time (Fig. 5*B*).

Hysteresis in the steady firing of medial rectus and abducens motoneurons during intersaccadic intervals was determined by plotting separately the relationship between firing rate and eye position 2 s after ON- and OFF-directed saccades. In four medial rectus and three abducens motoneurons, higher firing rates were reached for a given eye position after an ON-directed saccade than after an OFF-directed saccade (Fig. 5*C*). This feature yielded significantly different ($P < 0.05$) F_0 values in the rate-position relationships obtained in the two cases (8.2 ± 4 spikes/s, on the average). On the other hand, no significant variations were seen in the k-ON versus k-OFF values of each cell. Both slopes were obtained with high correlation coefficients ($r > 0.75$).

FIRING CHARACTERISTICS DURING SACCADES. All horizontal motoneurons fired a burst of spikes for saccades in the ON-direction, and the firing frequency decreased during every OFF-directed saccade. No qualitative variation was observed in this tonic-phasic schema, such as either phasic- or tonic-only motoneurons. Latency to saccades was similar for the three populations and was slightly higher for OFF-directed saccades. Average values were 14.1 ± 4.8 ms for ON-directed saccades and 20.2 ± 5.6 ms for OFF-directed saccades.

Eye velocity sensitivity during spontaneous saccades (r_s) was obtained as the slope of the rate-velocity plots. For a set of ≥20 saccades, the instantaneous firing rate was correlated to instantaneous eye velocity after subtraction of the eye position signal. Firing rate was shifted by the corresponding latency of the burst to the ensuing saccade. Figure 4, *D–F*, shows the rate-velocity regression lines for the three motoneuronal groups. Correlation coefficients were always >0.75. Mean eye velocity sensitivity was similar ($P > 0.4$) for the two subdivisions of the abducens nucleus [0.96 ± 0.44 (spikes/s)/(deg/s) for rostral and 1.03 ± 0.37 (spikes/s)/

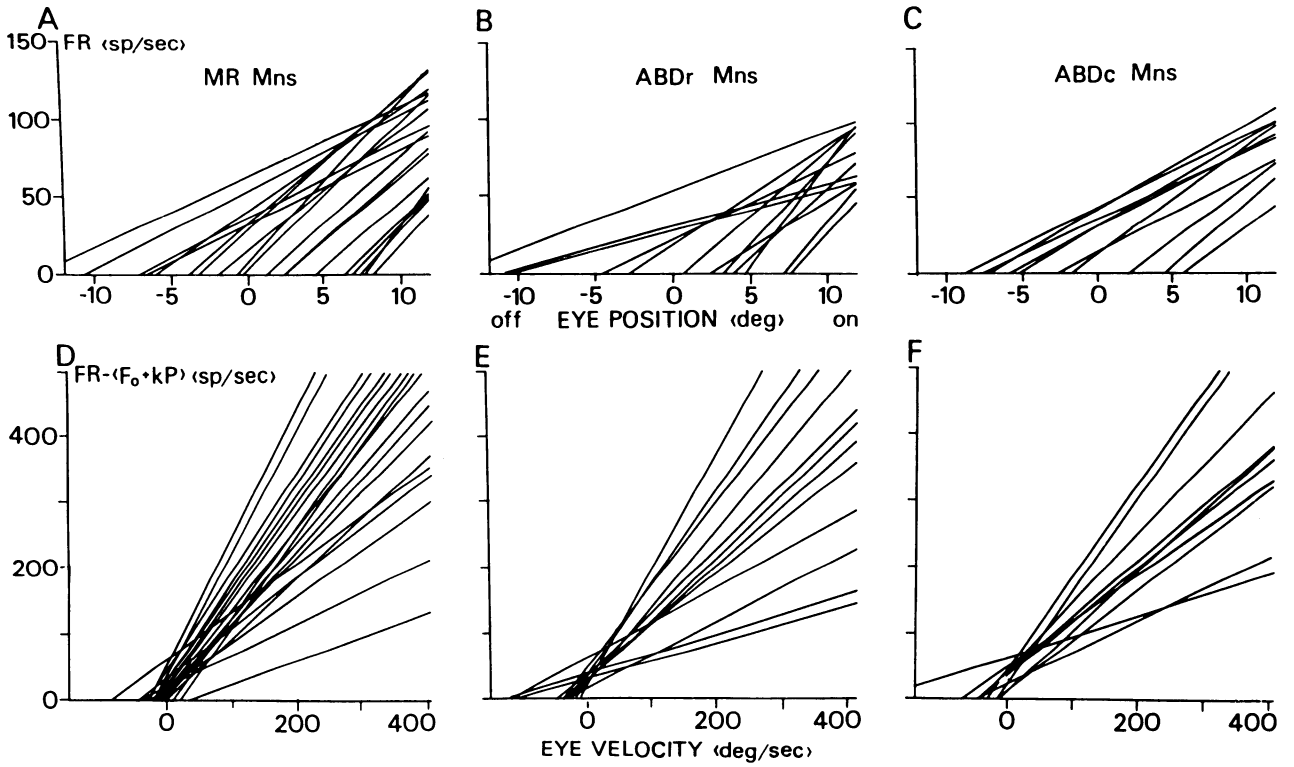

FIG. 4. Quantitative analysis of the firing frequency of horizontal extraocular motoneurons during spontaneous saccades and eye fixations. *A–C*: linear regression lines for the relationship between firing rate (FR) and eye position obtained for 19 sampled medial rectus (MR) motoneurons and 12 rostral (ABDr) and 10 caudal (ABDc) abducens motoneurons (Mns) during spontaneous eye movements. Correlation coefficients were >0.8. *D–F*: rate velocity relationships for the same motoneurons as in *A–C* obtained by linear regression of the firing rate minus the position component ($F_0 + kP$, see text) vs. eye velocity.

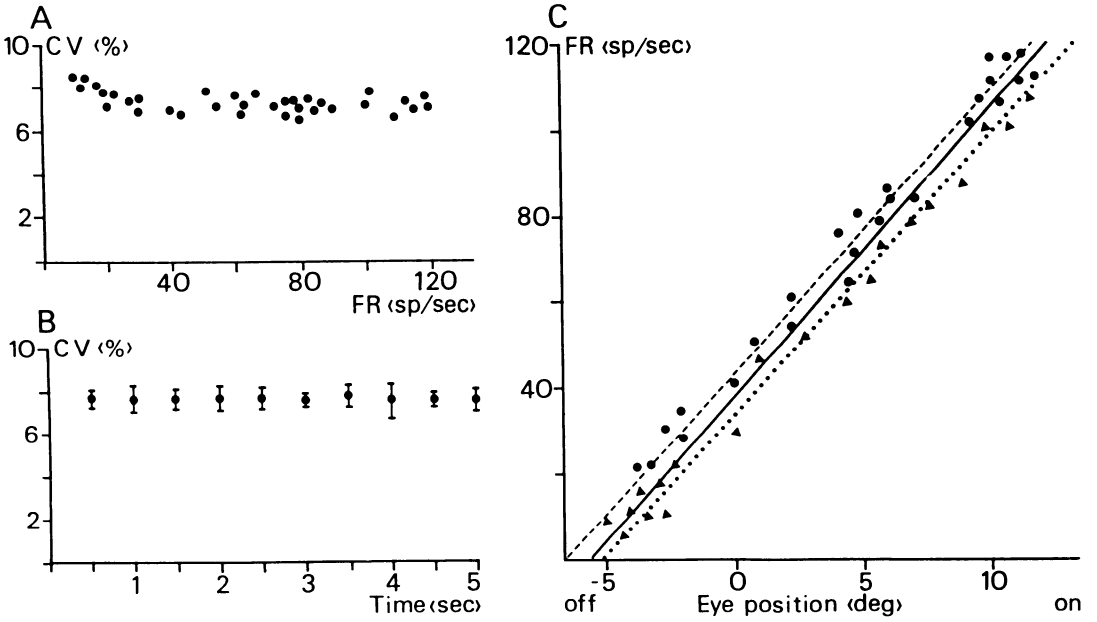

FIG. 5. Regularity of a medial rectus motoneuron firing rate during spontaneous intersaccadic periods. *A* and *B*: coefficient of variation (CV) as a function of the firing rate (FR) and time after the previous saccade, respectively. CV was calculated as the percent ratio of the standard deviation to the mean instantaneous firing rate. *C*: rate-position plots for intersaccadic intervals reached after ON saccades (●) (FR = 6.5 P + 43.5, r = 0.82, – – –), OFF saccades (▲) (FR = 6.35 P + 35.84, r = 0.81, · · · ·), and computed irrespective of the direction of the preceding saccade (FR = 6.78 + 39.2, r = 0.79, ——).

(deg/s) for caudal abducens motoneurons]. Medial rectus motoneurons exhibited the highest mean eye velocity sensitivity [1.19 ± 0.43 (spikes/s)/(deg/s)] although it was not significantly different ($P > 0.1$) on the whole for abducens motoneurons.

Firing rate did not reach the new steady level immediately after the end of the ON-directed saccade, but decayed gradually in an exponential-like manner (Figs. 2*A* and 3, *A* and *B*). Conversely, after an OFF-directed saccade, firing rate acquired the new tonic activity without appreciable transient changes (Fig. 3, *A* and *B*). Postsaccadic slide in the firing rate of motoneurons was characterized by the time constant of a single exponential function fitted by the least-squares procedure after subtracting the eye position and eye velocity components. Time constant of the slide ranged from 50 to 300 ms in the three groups of motoneurons. For a particular unit, the time constant of the slide changed in relation to the postsaccadic events. Saccades were followed by either stable eye positions or slow onward or backward drifts lasting up to 500 ms. The slow postsaccadic drift of eye position was quantified with the use of a pulse-step relationship measured as the percentage of the ratio $(P - S)/P$, where P and S were the pulse and the step, respectively (Optican and Miles 1985).

Figure 6, *A–C*, shows three examples of postsaccadic slide taken from a rostral abducens motoneuron during spontaneous eye movements. Larger time constants of the postsaccadic slide were associated with positive pulse-step relationships, that is, backward drifts; and shorter time constants were associated with onward drifts (Fig. 6*D*). Although there was a slight trend for saturation in both extremes of the scatter plot, linear regression lines for six motoneurons were obtained with correlation coefficients between 0.5 and 0.75.

DISCHARGE ASSOCIATED WITH BLINKS. The pattern of spontaneous eye movements of restrained goldfish was occasionally interrupted by a rather conspicuous eye movement named "stretch" or "blink" (Easter 1975). Blinks consisted of a fast (up to 400°/s) movement of both eyes, first in a temporal and downward direction and then in a nasal and upward direction (Fig. 7*A*). A clear retraction-like component was also observed, though not quantitated. The fast nasal component was shorter than the temporal component and was followed by a slow nasal drift (5–7°), lasting 2–4 s, that settled the eyes near center position in the orbit (Fig. 7*C*). Every motoneuron in the oculomotor and abducens nuclei showed an intense burst of spikes during the component of the blink corresponding to its respective ON-direction, and every motoneuron paused during the movement in the OFF-direction (Fig. 7, *A* and *B*).

Several motoneurons antidromically activated within the boundaries of the oculomotor nucleus did not show any spontaneous activity except for blinks. Some discharged during the initial fast velocity component and others during the second component. These motoneurons likely belonged to oculomotor nucleus subdivisions other than the medial rectus (Fig. 7*B*). Unexpectedly, motoneuronal discharge was not modulated during the long excursions of one or both eyes after blinks, but rather showed a fairly constant rate of 20–30 spikes/s, unrelated to eye position. The appropriate eye movement-related discharge was restored in coincidence with the appearance of a new saccade (Fig. 7*C*).

Response to vestibular stimulation

Passive sinusoidal head rotations in the dark produced compensatory eye movements, the peaks of which preceded those of the table position by 5–10° for all tested frequencies from $^1/_{16}$ to 4 Hz in octave intervals. Gain of the vestibuloocular reflex, measured as the ratio of peak eye velocity to peak head velocity in the dark, was nearly constant at different frequencies, being 0.79 ± 0.15 at $^1/_{16}$ Hz and 0.76 ± 0.17 at 4 Hz for 10 measures at each frequency.

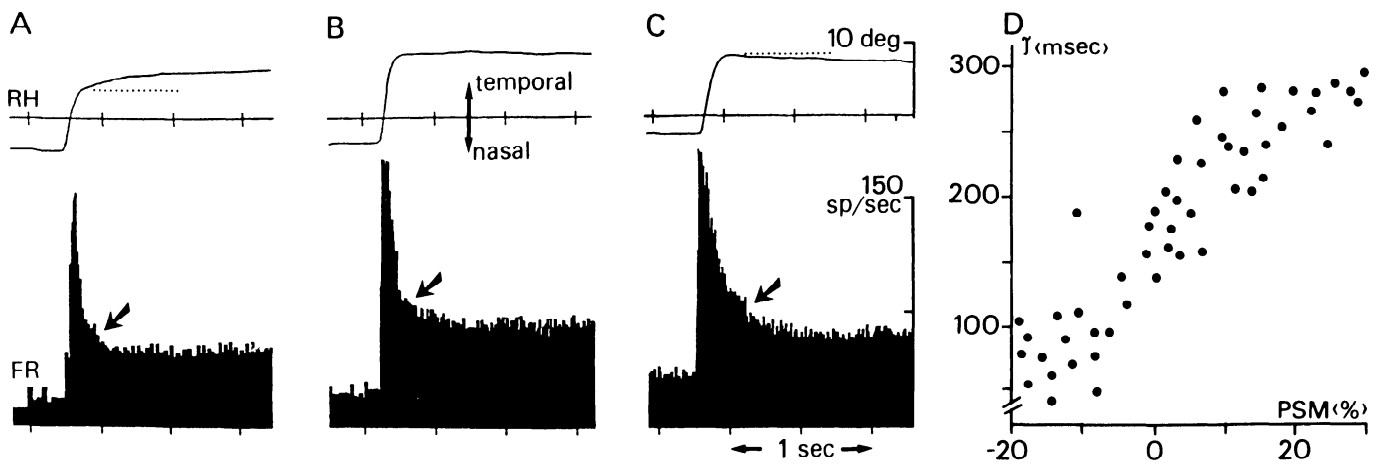

FIG. 6. Exponential decay of the firing rate (FR) after ON-directed saccades of a motoneuron recorded in the rostral subgroup of the abducens nucleus. *A–C*: 3 types of saccades illustrating the presence of onward (*A*) drifts, normal (*B*) termination of the saccade, and backward (*C*) drifts. Note the increase in the time course of the postsaccadic decay in the firing rate (arrows) from *A* to *C*. RH, right horizontal eye position. *D*: scatter plot showing that the single exponential time constant (τ) fitting the decay of firing rate after ON saccades is proportional to the percentage of eye position drift, i.e., the pulse-step mismatch (PSM). These data correspond to the motoneuron illustrated in *A–C*. PSM was calculated as the ratio $(P - S)/P$ in percentage, where P is the saccade amplitude and S the difference in position between the 2 consecutive intersaccadic periods.

Medial rectus and abducens motoneurons exhibited a sinusoidal modulation during head rotation, although they went into cutoff for a part of the cycle, according to their position threshold. During fast phases of vestibular nystagmus, motoneurons burst or paused for their ON- or OFF-directions, respectively.

Eye position (k_v) and eye velocity (r_v) sensitivity during vestibular stimulation were calculated by multivariate regression analysis at different frequencies, according to the first-order, single time constant, linear approximation (Skavenski and Robinson 1973). Firing rate, eye position, and eye velocity were displayed on a computer screen; and data were selected from 3 to 10 cycles. Higher-threshold motoneurons virtually only modulated sinusoidally at frequencies >1 Hz, when a spontaneous saccade displaced the eye toward the active field of the unit. For this reason, the available lowest-threshold units were largely analyzed and pooled. For rotational frequencies >1 Hz, the spontaneous pattern of scanning saccades was superimposed on the sinusoidal compensatory eye movements (Fig. 2*C*, *right*). For a total of seven medial rectus and five abducens motoneurons, calculation of eye position and velocity sensitivity could be achieved at all frequencies tested between 1/16 and 2 Hz. For the purpose of computing eye position and velocity sensitivity, fast phases of vestibular nystagmus and spontaneous saccades were manually removed with the help of cursors on the computer screen. In regard to eye position sensitivity, mean k_v at low frequencies (1/16 and 1/8 Hz) was lower by 10.8 and 12.1% than mean k_s for medial rectus and abducens motoneurons, respectively (Table 2). There was a general trend in every cell to exhibit higher k_v values with increasing frequency. As shown in Fig. 8*A* for medial rectus motoneurons, mean k_v was 42% higher at 2 than at 1/16 Hz. Similarly, for the abducens nucleus sample, mean k_v was 37% higher at 2 than at 1/16 Hz. The analysis of variance for repeated measurements of k_v data showed a significant ($P = 0.01$) positive linear trend. With respect to eye velocity sensitivity, similar values were obtained at all the frequencies tested for each unit (Fig. 8*B*). Thus no significant dependence was found for r_v with frequency; however, compared with r_s, r_v coefficients were higher by 18.8% for medial rectus motoneurons and 20% for abducens motoneurons (Table 2).

For each motoneuron, time constants (τ_v) were calculated as $\tau_v = r_v/k_v$ at every frequency. Because k_v values increased with frequency, mean time constants were ~25% lower at 2 than at 1/16 Hz. Figure 8*C* shows the phase lead for medial rectus motoneurons obtained by direct measurements from both the firing rate and eye position displays (asterisks) and by calculation from the mean time constant for each frequency (solid dots) according to the equation $\Phi = \arctan 2\pi f\tau_v$ (where Φ represents the phase lead and f

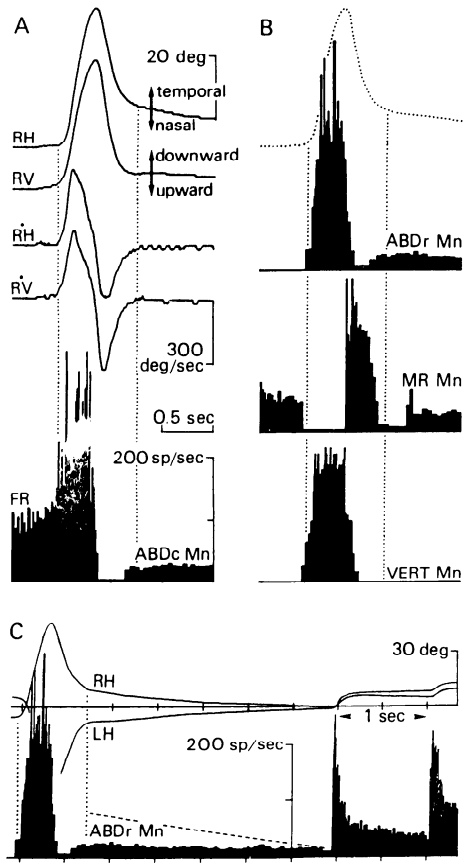

FIG. 7. *A* and *B*: discharge pattern of abducens and oculomotor motoneurons during the blink. Horizontal and vertical eye position (RH, RV) and velocity (RH, RV) during a typical blink are shown, and the dotted trace at the top of *B* is a copy of the RH trace in *A*. Caudal (ABDc Mn) and rostral (ABDr Mn) abducens motoneuron fired an intense burst of spikes during the temporalward part of the blink and paused during the nasalward component. A medial rectus (MR Mn) motoneuron firing in a symmetrical but antagonistic fashion is shown in *B*. Note the presence of a 2nd pause in the firing rate of the MRMn at the end of the nasalward fast component. Vertical motoneuron (VERT Mn) identified in the oculomotor nucleus was active only during the 1st fast component of the blink and remained silent during all other eye movements. *C*: after the blink (dotted vertical line to the *right*) the eye slowly drifted nasally. Note that during the drift the same ABDr Mn shown in *B* fired at a constant rate unrelated to eye position until the appearance of a new saccade. Dashed line corresponds to the expected firing rate of this motoneuron according to a 1st-order model.

TABLE 2. *Quantitative characteristics of identified horizontal extraocular motoneurons* obtained during spontaneous eye movements and head rotation*

Parameter	Source of Motoneurons: Medial rectus	Rostral abducens	Caudal abducens
Position gain during intersaccadic periods (k_s), spikes · s^{-1} · deg^{-1}	6.02 ± 1.21	4.91 ± 0.99	4.70 ± 0.42
Position gain during the slow phase of the VOR at 1/8 Hz (k_v), spikes · s^{-1} · deg^{-1}	5.40 ± 1.25	4.32 ± 0.92	4.10 ± 0.30
Velocity gain during spontaneous saccades (r_s), spikes · s^{-1} · deg^{-1}	0.99 ± 0.28	0.67 ± 0.21	0.79 ± 0.25
Velocity gain during the slow phase of the VOR at 1/8 Hz (r_v), spikes · s^{-1} · deg^{-1}	1.22 ± 0.30	0.80 ± 0.26	0.96 ± 0.31
$\tau_s = r_s/k_s$ at 1/8 Hz, ms	166.6 ± 40	136.4 ± 39	164.3 ± 39
$\tau_v = r_v/k_v$ at 1/8 Hz, ms	226.2 ± 65	186.3 ± 48	230.7 ± 59
$\tau_0 = \tan\phi/2\pi f$ at 1/8 Hz, ms	249.8 ± 57	197.2 ± 51	245.7 ± 30

Values are mean ± SD. VOR, vestibuloocular reflex. *Motoneurons were selected for low recruitment threshold.

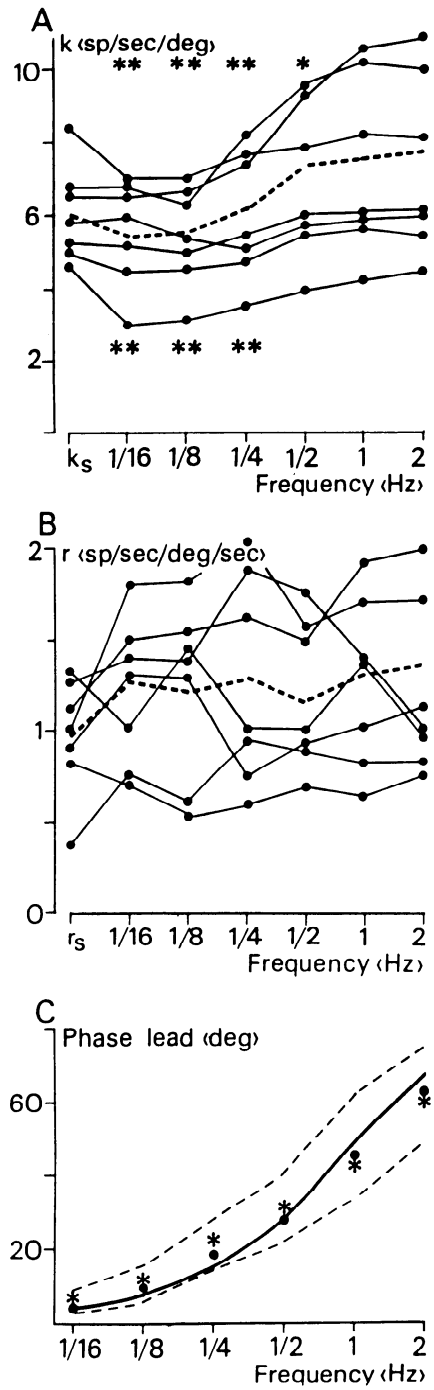

FIG. 8. Analysis of the behavior of 7 identified medial rectus motoneurons during sinusoidal vestibular stimulation. *A*: eye position sensitivity (k_v) for each neuron during sinusoidal vestibular stimulation, measured at frequencies spaced by octaves from 1/16 to 2 Hz. Dashed line represents mean values for all cells. Mean eye position sensitivity during spontaneous eye movements (k_s) is also shown for comparison. Significant differences with k_v values obtained at 2 Hz are indicated at the *top* of the figure (**$P < 0.01$; *$P < 0.05$). Significant differences with k_s values are shown at the *bottom*. *B*: same for r_v and r_s values; r_s and r_v represent the eye velocity during spontaneous eye movements and in response to vestibular stimulation, respectively. *C*: phase shift diagrams for the sampled medial rectus motoneurons. Area between dashed lines corresponds to the range of phase leads obtained directly from the instantaneous firing rate and eye position displays. Asterisks are mean values of the latter. Solid dots are mean phase shifts calculated from the time constant ($\tau_v = r_v/k_v$) of each medial rectus motoneuron. Solid line is the 1st-order approximation obtained from $\tau_s = r_s/k_s$ for the same set of motoneurons.

the test frequency). These two sets of data showed little difference compared with the first-order bode plot (solid line) computed with the use of the mean time constant obtained during spontaneous eye movements ($\tau_s = r_s/k_s$). As illustrated in Fig. 8*C*, phase leads at frequencies <1/2 Hz were higher than those predicted by the first-order approximation. Although it was less noticeable, the opposite occurred for frequencies >1/2 Hz. Linearization of the bode plots and regression by the least-squares method revealed the existence of at least two slopes that better described the relationship between tanΦ and the pulsation ($w = 2\pi f$ in rad/s) over the range of studied frequencies. However, single-slope fitting also yielded high correlation coefficients ($r \geq 0.8$ for direct phase measurements and $r \geq 0.83$ for predictions from τ_v). Table 2 summarizes the values of the time constants τ_s and τ_v at 1/8 Hz and τ_0 for medial rectus and abducens motoneurons. The latter was calculated from direct measurements of firing rate phase shift, solving the above equation as $\tau_0 = \tan\Phi/2\pi f$ at 1/8 Hz. As expected from the phase shift diagrams, τ_v and τ_0 at this frequency were significantly higher ($P < 0.05$) than τ_s, and the reverse occurred at frequencies >1/2 Hz.

Behavior during optokinetic stimulation and visual-vestibular interactions

Sinusoidal optokinetic stimulation produced a sinusoidal pattern of eye movements, the gain of which was ~0.6 at 1/16 and 1/8 Hz and then fell abruptly at higher frequencies (gain <0.3 at 1/4 Hz). The firing rate of every motoneuron was also modulated during optokinetic stimulation (Fig. 2*B*). Position and velocity sensitivity were mainly measured at 1/8 Hz. In four medial rectus and four abducens motoneurons, mean position and velocity sensitivity during optokinetic and vestibular stimulation showed similar values ($P > 0.1$). Individual differences in motoneuronal position and velocity sensitivity for visual and vestibular stimuli were within 2.4–6 and 1.7–7.5% for medial rectus and abducens motoneurons, respectively.

Figure 9 illustrates an example of vestibular stimulation in the dark, followed by a period of suppression of the vestibular response when the visual world moved with the same velocity and direction as the head (required eye movement gain was equal to 0). During the suppression period, motoneuronal firing rate was modulated in response to neither vestibular nor optokinetic stimulation. Instead, a monotonic activity proportional to eye position was present. Saccades also occurred during the suppression paradigm. Eye movement gains >1 were obtained by oscillating the visual world at higher speed than the head rotation and 180° out of phase. In this case, the discharge rate of motoneurons was deeply modulated in relation to eye position and velocity. The k_v and r_v values were similar ($P > 0.1$) to those obtained during either pure vestibular or optokinetic stimulation.

Relationships between motoneuronal parameters

Correlations between several parameters, such as position and velocity sensitivity, recruitment threshold, and antidromic activation latency, were carried out within each

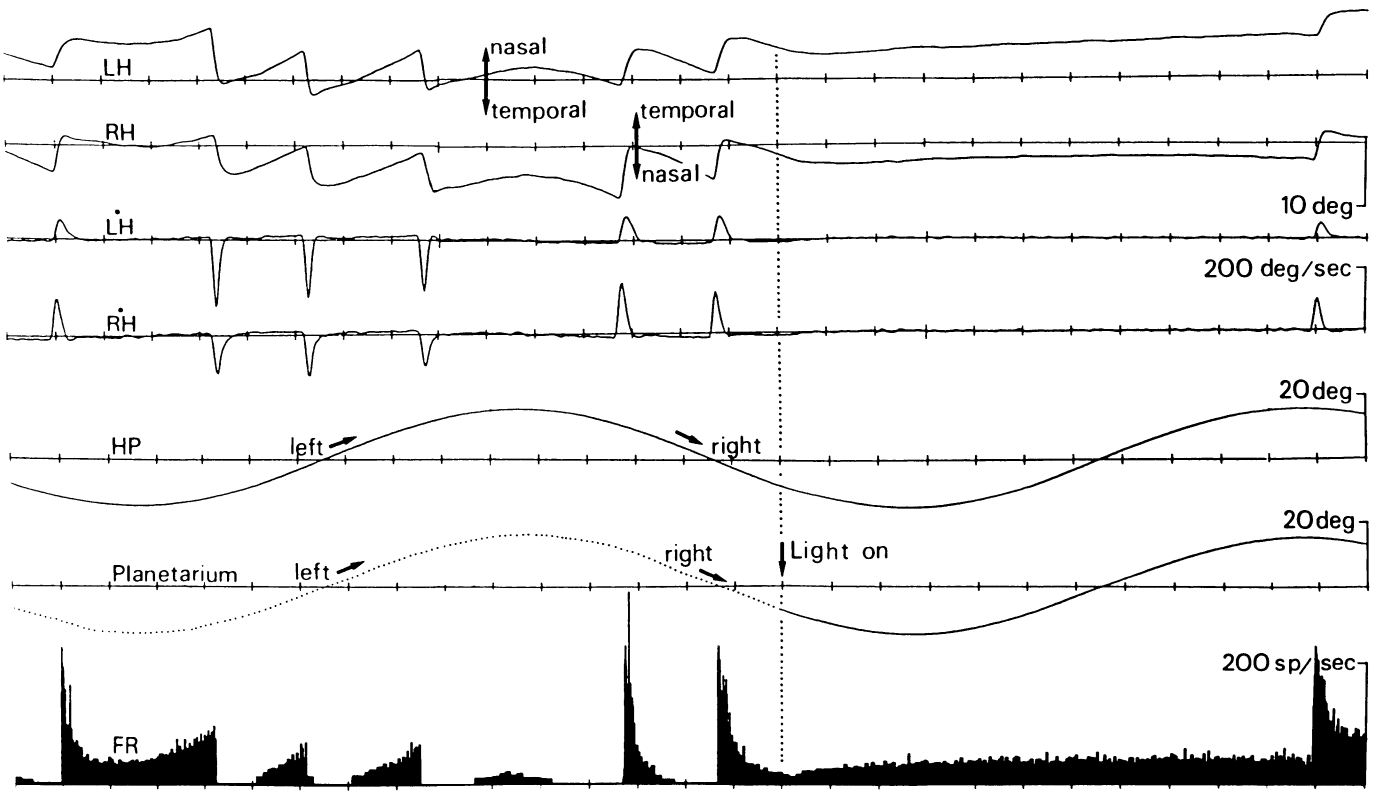

FIG. 9. Response of a caudal abducens motoneuron during suppression of the vestibuloocular reflex. Vestibular nystagmus and sinusoidal modulation of the motoneuron in response to sinusoidal head rotation in the dark were abolished when the visual world moved (downward arrow) at the same velocity and direction as the turntable. Planetarium frame was connected to the turntable. LH, RH, $\dot{LH}$, and $\dot{RH}$ are left and right horizontal eye position and velocity, respectively. HP, head position.

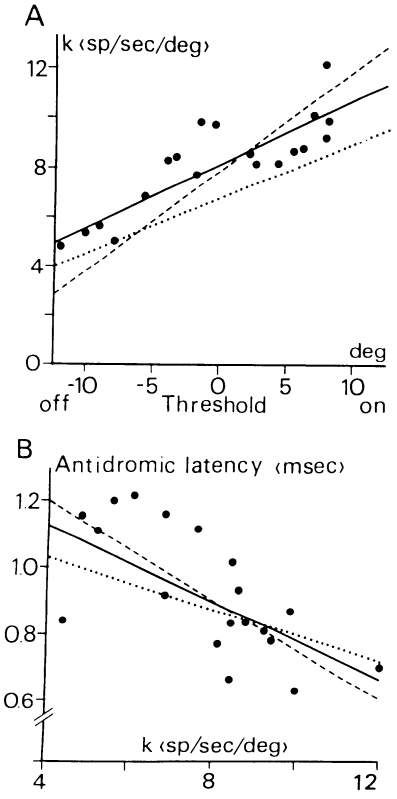

motoneuronal group to ascertain whether differences in excitability could be related to inferred cell size. Results depicted in Fig. 4, *A–C*, indicated that motoneurons with the lower-position thresholds tended to have lower slopes in the rate-position relationships. Values for k_s plotted against position threshold yielded significant relationships ($P < 0.01$) for the three motoneuronal populations ($r > 0.8$; see Fig. 10*A*). Weaker relationships ($r > 0.61$), although significant ($P < 0.05$), were obtained between r_v at ⅛ Hz and unit position threshold.

To assess whether motoneuronal recruitment could be expressed as a function of cell size, antidromic latency was assumed to be an index of cell size, and this characteristic was correlated with eye position sensitivity and unit position threshold. A weak inverse relationship (r ranged from −0.48 to −0.62, $P < 0.05$) was found between antidromic

FIG. 10. *A*: relationship between eye position sensitivity (k_s) during spontaneous eye movements and eye position threshold for medial rectus motoneurons (●). Linear regression line (——) was $k_s = 0.24\text{THR} + 8.27$ ($r = 0.82$). Linear regression lines are also shown for rostral abducens ($k_s = 0.41\text{THR} + 7.90$, – – –) and caudal abducens ($k_s = 0.22\text{THR} + 6.73$, · · · ·) motoneurons. Coefficients of correlation were $r = 0.81$ and 0.8, respectively. *B*: relationships between latency to the 1st negative peak of the antidromically evoked spike and k_s. For medial rectus (●) motoneurons, the linear regression line (——) was $L = -0.057k_s + 1.38$; $r = -0.62$; for rostral abducens, $L = -0.051k_s + 1.19$ (– – –); and for caudal abducens, $L = -0.068k_s + 1.46$ (· · · ·). Correlation coefficients for regression lines were $r = -0.48$ for rostral and −0.51 for caudal abducens motoneurons.

latency and eye position sensitivity (Fig. 10*B*). The correlations obtained between antidromic latency and threshold (r ranged from -0.22 to -0.41) for the three motoneuronal groups were not significant ($P > 0.1$).

DISCUSSION

Discharge pattern of medial rectus and abducens motoneurons

The most general conclusion from this study is that all medial rectus and abducens motoneurons in goldfish exhibit a burst of spikes for their respective ON-directed saccades and a tonic firing proportional to eye position when the latter exceeds motoneuronal recruitment threshold. No qualitative variation in the above pattern was found for motoneurons of either nuclei. These basic firing properties are similar to those reported for medial rectus and abducens motoneurons in both cat and monkey (De la Cruz et al. 1989; Delgado-García et al. 1986a; Fuchs et al. 1988; Robinson 1970) and to those named P type in the oculomotor complex of the goldfish (Hermann 1971).

By contrast, the data presented here are not in agreement with unidentified abducens motoneurons recorded in the goldfish (Gestrin and Sterling 1977). Abducens motoneurons of the rostral subgroup were not reported to discharge for ON-directed saccades, and their maximum tonic firing rate range was 10–20 spike/s. The putative tonic motoneurons were suggested to innervate the smaller and slow fibers of the lateral rectus muscle. However, purely tonic motoneurons were not recorded in the rostral subdivision of the abducens nucleus on the basis of antidromic identification criterion. Thus it is concluded that both the rostral and caudal subgroups of abducens motoneurons share the same qualitative firing pattern.

The assumption that the two abducens subdivisions separately innervate different types of muscle fibers of the abducens muscle (Gestring and Sterling 1977) also seems less plausible in light of the mechanical studies in the extraocular muscles of catfish, a teleost with a subdivided abducens nucleus (Lennerstrand and Baker 1987). The later work showed similar mechanical properties in the lateral rectus muscle after selective stimulation of the two abducens nerve branches at their exit from the brain stem.

Both fast- and slow-fiber muscle types have been described in the six extraocular muscles of fish (Davey et al. 1975; Easter 1979; Kumari et al. 1979; Sterling 1977). A cytochemical study of carp extraocular muscles (Kumari et al. 1979) revealed the medial rectus muscle to contain the highest percentage (48%) of tonic (slow) muscle fibers; however, neither the present data nor those of others (Hermann 1971; Korn and Bennett 1975) have reported purely tonic motoneurons in the medial rectus pool. Consequently, the present results further suggest that a gradation, rather than a division, of labor underlies the composition of position and velocity signals in the goldfish medial rectus and abducens motoneurons. This organizational principle is also the case for mammals (De la Cruz et al. 1989; Delgado-García et al. 1986a; Fuchs et al. 1988; Robinson 1970).

Firing properties during spontaneous eye movements

The rather stereotyped pattern of spontaneous eye movements in a restrained goldfish contrasts with the rich repertoire found during active swimming and in response to various environmental stimuli (Easter and Johns 1974; Graf and Meyer 1978). Eye movements during head fixation were restricted to the horizontal plane. Although not extensively examined in the present work, the eye appeared to be held passively in a vertical "neutral" position, because no units other than medial rectus fired within the electrophysiological limits of the oculomotor nucleus. Identified motoneurons that were silent during horizontal eye movements and that fired in correlation to either the downward or upward direction of eye blinks were considered as belonging to oculomotor nucleus subdivisions other than medial rectus. The fact that the scanning eye movements in the restrained goldfish also occurred in the dark and in the absence of other stimuli, such as lateral line and vestibular inputs, demonstrates the presence of a central pattern generator. In curarized goldfish, abducens motoneurons continue to fire in a phasic-tonic manner resembling the pattern in the unparalyzed preparation (Gestrin and Sterling 1977).

Mean values for k_s and r_s were higher for medial rectus than for abducens motoneurons. This finding could not be ascribed to a bias in the sample of units between both nuclei, because the distribution and mean values of thresholds, as well as the range of eye position and velocity sensitivity, were similar between the two nuclei. These results may be explained by differences in motoneuronal excitability and/or afferent organization.

Differences in mean k_s and r_s values between both motoneuronal pools might be related to the asymmetries reported at the level of the muscle and the motor nuclei in teleosts. The lateral rectus muscle is larger than the medial rectus muscle in cross section. It is also twice as long and exhibits a greater number of fibers (Graf and McGurk 1985). The lateral rectus muscle contains a larger proportion (65%) of fast fibers than the medial rectus muscle (52%; Kumari et al. 1979). In addition, there is a greater number of motoneurons in the abducens nucleus than in the medial rectus subdivision of the oculomotor complex (Graf and McGurk 1985; this study). Thus higher k_s and r_s values in the medial rectus population are in the appropriate direction to compensate for an imbalance (i.e., asymmetry) in the production of tension between the agonist-antagonist muscle pair. However, to assess this hypothesis properly, the contractile properties of individual motor units should be measured to determine the amount of force per motor unit and thus to compute the total force exerted by the muscle as well as the mechanical constants of the orbital tissues.

The average k_s and r_s values obtained in our experiments were similar to those described for medial rectus and abducens motoneurons in cats and monkeys (De la Cruz et al. 1989; Delgado-García et al. 1986a; Skavenski and Robinson 1973); however, the ranges were wider in mammals, especially in the direction of higher values. The lower numerical constants in goldfish might be expected from their

relatively slower eye movements and narrower oculomotor range.

The stationary firing rate of motoneurons was influenced by the direction of the preceding saccade. This phenomenon was first referred to by Eckmiller (1974) as a static hysteresis and was later observed by others (Delgado-García et al. 1986a; Goldstein and Robinson 1986). The present data suggest a constant difference of ~10 spikes/s over most of the oculomotor range in the rate-position plots obtained after ON- or OFF-directed saccades. Differences in slope were found when data were not evenly distributed along the oculomotor range for the ON- and OFF-directions. The latter probably reflects the fact that linear regressions are not always the best fit to the data (Delgado-García et al. 1986a). This discrepancy in the firing rate after ON- and OFF-directed saccades could not be attributed to the transient slow decrease in the firing rate after the saccade, because measures of steady-state rate were taken after 2 s and the time constant of the postsaccadic slide was roughly between 50 and 300 ms. Thus it seems that a real static hysteresis is present in the behavior of goldfish motoneurons during the maintenance of eye position. It has been suggested that hysteresis in the motoneuron discharge might cancel out the mechanical hysteresis observed in the extraocular muscle (Collins 1975).

Vestibular behavior and postsaccadic slide

Bode phase plots of goldfish medial rectus and abducens motoneurons obtained either by direct measurements of firing rate and eye position or by computations from τ_v during vestibular stimulation had a characteristic frequency (the cutoff frequency of a 1st approximation) similar to that reported for monkey (Skavensky and Robinson 1973) and cat (Delgado-García et al. 1986a). The data presented here, however, exhibit a lower slope compared with a first-order approximation (τ_s), but the difference is not as marked as that reported in the cat (Goldberg 1980) and monkey (Fuchs et al. 1988). A less steep bode plot has been modeled as being produced by a zero in the transfer function of the motoneuronal pool (Fuchs et al. 1988) and the orbital mechanics (Robinson 1964), likely compensating each other during the normal repertoire of eye movements. The presence in the goldfish data of an exponential-like decay in the firing rate after the end of a saccade, and the inverse dependence of the neuronal time constant (τ_v) on frequency, support Robinson's conclusion that the oculomotor plant would be modeled better by linear higher-order approximations (Robinson 1964). For a sudden transient change in eye velocity (i.e., a saccade), it could be argued that the postsaccadic slide represents the action of a frequency-dependent filter acting in parallel with the pure eye position and eye velocity signals. Similarly, during phase analysis in the frequency domain, this filter could also produce the delay in the rate of phase change with frequency. Whether these two phenomena can be generalized as the result of the same mechanism still needs to be explored.

The present results demonstrate a relationship between the time constant of the exponential decay of firing rate after the saccade and the postsaccadic events in eye position. These results imply that the neural slide signal is in fact coding the transition to the new eye position. The saccadic undershoots and overshoots were common in the normal pattern of eye movements in goldfish, and these responses have been shown to be independent of direction and idiosyncratic laterality (Easter 1975). The postsaccadic slide has been modeled as a third element in the motoneuronal command, in addition to the pulse and the step, to account for the postsaccadic adaptability in monkeys exposed to retinal image slip immediately after the saccade (Optican and Miles 1985). The origin of this neuronal slide is uncertain. It is likely not generated solely at the motoneuronal pool, because the usual membrane adaptation to current pulses would yield smaller time courses than those of the postsaccadic slide (Durand 1989; Grantyn and Grantyn 1978). Besides, the slide has been observed in premotor neurons projecting to oculomotor and abducens nuclei (Delgado-García et al. 1986b, 1989; Iwamoto et al. 1990). Taken together, these data suggest that the slide is generated in premotor networks conveying position and velocity signals to the motoneuron. However, the possible role of motoneuronal membrane adaptation in the generation of the postsaccadic slide cannot be completely discarded, as judged from the large adaptation time constants described for cat abducens and trochlear motoneurons when stimulated intracellularly with current steps (Baker and Precht 1972; Barmack 1974).

The parameters of a first-order approximation vary with the stimulus frequency in mammalian extraocular motoneurons (De la Cruz et al. 1989; Fuchs et al. 1988; Stahl and Simpson 1988). In addition, a second source of variation in fish oculomotor mechanics is temperature. Our experiments were performed at 20°C, which was within 1°C of the acclimation temperature. The first-order approximation obtained from τ_s had a cutoff frequency close to that reported for other teleosts at similar temperatures (Montgomery and MacDonald 1985). However, as the result of an increased viscosity and decreased elasticity with lower temperatures, an inverse relationship exists between cutoff frequency and temperature (Montgomery and MacDonald 1985; Montgomery and Paulin 1984). Because the first-order approximation of the dogfish oculomotor mechanics measured at 14°C (Montgomery 1983) seems to have even a lower slope than that found for the goldfish at 20°C, it would be of interest to correlate the relative variation of these parameters with temperature while evaluating presumed effect on motoneuronal time constant to match the new mechanical situation of the orbital tissues.

Blinks

A retractor bulbi muscle is present in lampreys and all tetrapod classes; however, neither teleosts nor elasmobranchs have this retractor muscle (Fritzsch et al. 1990). The retractor muscle is not the only way of producing an eye retraction, because retraction-like responses, presumably due to cocontraction of eye muscles, have been found in elasmobranchs (Bell and Satchell 1963) and puffers (Korn and Bennett 1975). A certain degree of synergism also occurs in the cat lateral rectus muscle because of the

activation of a small (10%) percentage of abducens motoneurons that burst during eye retraction (Delgado-García et al. 1990). The blink eye movement of goldfish resembles a retraction-like response, but its occurrence does not seem to be correlated to any behavioral situation, nor can it be evoked as a short-latency reflex response. Furthermore, the blink was shown to be produced by a sequential, not simultaneous, discharge of motoneurons and muscle contraction. Thus active forward and backward movements about the vertical and horizontal axes accompanied eye retraction. The behavioral significance of this eye movement in teleosts is unclear. The only context in which the eyes are retracted simultaneously in the orbit is during the escape response initiated by visual, acoustic, and lateral line stimulation. A disynaptic circuit mediates this response, which is triggered by a single action potential in the Mauthner cell (Faber et al. 1989). It is not known whether interneurons in this circuit are active in the production of a blink.

One possible explanation for the drift in eye position after the blink is to attain a centered position of the eyes in the orbit. Because both the medial rectus and abducens motoneurons fired at a constant rate of 20–30 spike/s, the eye would reach a position at which the forces exerted by the medial and lateral rectus muscles are in equilibrium. From this viewpoint, the blinks could be proposed as a mechanism that controls both individual eye position and the angle between the two eyes. However, monocular or dysmetric saccades also have been suggested as mechanisms by which goldfish establish vergence angle (Easter 1971).

Optokinetic response and visual-vestibular interactions

The behavior of motoneurons during optokinetic and vestibular stimulation showed no variation between the firing-related parameters (k and r). In addition, during visual-vestibular interactions, motoneuronal firing rate correctly predicted the actual eye movement, rather than showing differences due to the relative contributions of vestibular and optokinetic inputs to the motoneuron. These two quantitative observations suggest that the optokinetic and vestibular pathways share a common premotor relay. The existence of separate inputs to the motoneuron of exactly the same synaptic efficacy could also explain the similar k and r coefficients for the two responses. Optokinetic pathways to the motoneurons are poorly described in teleosts; yet optokinetic velocity signals have been found in vestibular neurons of the goldfish (Allum et al. 1976). The latter finding suggests that velocity information arrives at motoneurons already combined from premotor neurons.

Neuronal correlates to recruitment order

Recruitment order within pools of spinal motoneurons has been described as rather fixed and explained by differences in excitability that are correlated to motoneuronal size (Henneman et al. 1965). Henneman's size principle has been widely discussed (Burke 1981; Desmedt and Godaux 1981; Stein and Bertoldi 1981; Ulfhake and Kellerth 1982), especially in regard to the variations of motoneuronal recruitment threshold described for different synaptic inputs. In cat abducens motoneurons, input resistance was inversely correlated with axonal conduction velocity (Grantyn and Grantyn 1978). Because conduction velocity indirectly represents cell size, this measurement establishes a relationship between excitability and size. In the present work, firing frequency during tonic discharge (k_s) and rate modulation during a graded velocity input (r_v) were interpreted for each motoneuron as (indirect) measurements of excitability.

Relationships obtained between k_s and r_v with threshold revealed the existence of a certain degree of recruitment in both medial rectus and abducens motoneuron pools. Those neurons with high position and velocity sensitivity tended to initiate discharge in association with more eccentric eye positions. Similar data have been reported for monkey (Fuchs et al. 1988), cat (Delgado-García et al. 1986a), and goldfish (Gestrin and Sterling 1977) abducens motoneurons. The goldfish data indicate that recruitment order is established similarly for different commands conveyed to a particular group of motoneurons. However, it is not yet known, in teleosts, whether the same source of afferents transmits both eye position and velocity signals to the motoneuron and/or the synaptic weight of the possible diverse inputs. An important issue is whether the relationship between rate-position slope and threshold is also present in premotor neurons projecting to oculomotor motoneurons, as described for cat vertical eye movement–related secondary vestibular neurons (Iwamoto et al. 1990) and cat abducens internuclear neurons (Delgado-García et al. 1986b). A similar organization was not found for monkey internuclear neurons (Fuchs et al. 1988). In goldfish, the antidromic latencies failed to produce good correlations to rate-position slopes (k_s). In addition, the relationships between latency and threshold, although inversely correlated, were found not to be significant for medial rectus and abducens motoneurons. For cat abducens neurons, weak relationships were described between latency and eye position sensitivity (Delgado-García et al. 1986a,b). By contrast, in monkey, no relationship was found between threshold and latency for abducens motoneurons and interneurons (Fuchs et al. 1988). Thus the present data and the results of others in several species suggest that a recruitment order based exclusively on a size principle seems not to be a sufficient criterion for ranking the motoneuronal pool as a function of firing-related parameters. Nevertheless, the size principle implies that, if cells with high threshold are more excitable, they should be expected to exhibit higher firing rates. Our results point just in that direction, because k_s and r_v were directly related to threshold.

Absence of correlation between the size variation and the density of synaptic inputs has been reported for goldfish abducens motoneurons (Sterling 1977). Thus, as indicated by present physiological and previous morphological data, the recruitment pattern within the goldfish oculomotor system cannot be solely a consequence of variation in cell size. Factors such as differences in passive and active membrane properties and in the arrangement of synaptic inputs between individual motoneurons must also play important roles.

This work was partly supported by grants from the Comisión Interministerial de Ciencia Y Tecnología in Spain, the Spain-USA Joint Committee, and National Eye Institute Grant EY-02007. A. Pastor was a scholar of the FISSS.

Address for reprint requests: R. Baker, Dept. of Physiology and Biophysics, New York University Medical Center, New York, NY 10016.

Received 11 April 1991; accepted in final form 23 July 1991.

REFERENCES

ALLUM, J. H. J., GRAF, W., DICHGANS, J., AND SCHMIDT, C. L. Visual-vestibular interactions in the vestibular nuclei of the goldfish. *Exp. Brain Res.* 26: 463–485, 1976.

ALLUM, J. H. J., GREEFF, N. G., AND TOKUNAGA, A. Projections to the rostral and caudal abducens nuclei in the goldfish. In: *Progress in Oculomotor Research,* edited by A. F. Fuchs and W. Becker. New York: Elsevier, 1981, vol. 12, p. 253–262.

BAKER, R. AND PRECHT, W. Electrophysiological properties of trochlear motoneurons as revealed by IVth nerve stimulation. *Exp. Brain Res.* 14: 127–157, 1972.

BARMACK, N. H. Saccadic discharges evoked by intracellular stimulation of extraocular motoneurons. *J. Neurophysiol.* 37: 395–412, 1974.

BELL, J. P. AND SATCHELL, G. H. An undescribed unilateral ocular reflex in the dogfish *Squalus acanthias. Austr. J. Exp. Biol.* 41: 221–234, 1963.

BURKE, R. E. Motor unit recruitment: what are critical factors? In: *Progress in Clinical Neurophysiol. Motor Unit Types, Recruitment and Plasticity in Health and Disease,* edited by J. E. Desmedt. Basel: Karger, 1981, vol. 9, p. 61–84.

COLLINS, C. C. The human oculomotor control system. In: *The Basic Mechanisms of Ocular Motility and Their Clinical Implications,* edited by G. Lennerstrand and P. Bach-y-Rita. Oxford, UK: Pergamon, 1975, p. 145–180.

CULLHEIM, S. Relations between cell body size, axon diameter and axon conductivity in the cat sciatic motoneurons stained with HRP. *Neurosci. Lett.* 8: 17–20, 1978.

DAVEY, D. F., MARK, R. F., MAROTTE, L. R., AND PROSKE, U. Structure and innervation of extraocular muscles of *Carassius. J. Anat.* 120: 131–147, 1975.

DE LA CRUZ, R. R., ESCUDERO, M., AND DELGADO-GARCÍA, J. M. Behaviour of medial rectus motoneurons in the alert cat. *Eur. J. Neurosci.* 1: 288–295, 1989.

DELGADO-GARCÍA, J. M., DEL POZO, F., AND BAKER, R. Behavior of neurons in the abducens nucleus of the alert cat. I. Motoneurons. *Neuroscience* 17: 929–952, 1986a.

DELGADO-GARCÍA, J. M., DEL POZO, F., AND BAKER, R. Behavior of neurons in the abducens nucleus of the alert cat. II. Internuclear neurons. *Neuroscience* 17: 953–973, 1986b.

DELGADO-GARCÍA, J. M., EVINGER, C., ESCUDERO, M., AND BAKER, R. Behavior of accessory abducens motoneurons during eye retraction and rotation in the alert cat. *J. Neurophysiol.* 64: 413–422, 1990.

DELGADO-GARCÍA, J. M., VIDAL, P. P., GÓMEZ, C., AND BERTHOZ, A. A neurophysiological study of prepositus hypoglossi neurons projecting to oculomotor and preoculomotor nuclei in the alert cat. *Neuroscience* 29: 291–307, 1989.

DESMEDT, J. E. AND GODAUX, E. Spinal motoneuron recruitment in man: rank deordering with direction but not with speed of voluntary movement. *Science Wash. DC* 214: 933–936, 1981.

DIERINGER, N. AND PRECHT, W. Functional organization of eye velocity and eye position signals in abducens motoneurons of the frog. *J. Comp. Physiol.* 158: 179–194, 1986.

DURAND, J. Intracellular study of oculomotor neurons in the rat. *Neuroscience* 30: 639–649, 1989.

EASTER, S. S. Spontaneous eye movements in restrained goldfish. *Vision Res.* 11: 333–342, 1971.

EASTER, S. S. The time course of saccadic eye movements in goldfish. *Vision Res.* 15: 405–409, 1975.

EASTER, S. S. The growth and development of the superior oblique muscle and trochlear nerve in juvenile and adult goldfish. *Anat. Rec.* 195: 683–698, 1979.

EASTER, S. S. AND JOHNS, P. R. Horizontal compensatory eye movements in goldfish (*Carassius auratus*). II. A comparison of normal and deafferented animals. *J. Comp. Physiol.* 92: 37–57, 1974.

ECKMILLER, R. Hysteresis in the static characteristics of eye position coded neurons in the alert monkey. *Pfluegers Arch* 350: 249–258, 1974.

FABER, D. S., FETCHO, J. R., AND KORN, H. Neuronal networks underlying the escape response in goldfish. General implications for motor control. *Ann. NY Acad. Sci.* 563: 11–33, 1989.

FUCHS, A. F. AND LUSCHEI, E. S. Firing patterns of abducens neurons of alert monkeys in relationship to horizontal eye movement. *J. Neurophysiol.* 33: 382–392, 1970.

FUCHS, A. F., SCUDDER, C. A., AND KANEKO, C. R. S. Discharge patterns and recruitment order of identified motoneurons and internuclear neurons in the monkey abducens nucleus. *J. Neurophysiol.* 60: 1874–1895, 1988.

FRITZSCH, B., SONNTAG, R., DUBUC, R., OHTA, Y., AND GRILLNER, S. Organization of the six motor nuclei innervating the ocular muscles in the lamprey. *J. Comp. Neurol.* 294: 491–506, 1990.

GESTRIN, P. AND STERLING, P. Anatomy and physiology of goldfish oculomotor system. II. Firing patterns of neurons in abducens nucleus and surrounding medulla and their relation to eye movements. *J. Neurophysiol.* 40: 573–588, 1977.

GOLDBERG, J. *Activity of Abducens Nucleus Neurons in the Alert Cat* (PhD dissertation). Berkeley, CA: Univ. of California, 1980.

GOLDSTEIN, H. P. AND ROBINSON, D. A. Hysteresis and slow drift in abducens unit activity. *J. Neurophysiol.* 55: 1044–1056, 1986.

GRAF, W. AND BAKER, R. The vestibuloocular reflex of the adult flatfish. I. Oculomotor organization. *J. Neurophysiol.* 54: 887–899, 1985.

GRAF, W. AND MCGURK, J. F. Peripheral and central oculomotor organization in the goldfish, *Carassius auratus. J. Comp. Neurol.* 239: 391–401, 1985.

GRAF, W. AND MEYER, D. L. Eye position in fishes suggest different modes of interaction between commands and reflexes. *J. Comp. Physiol.* 128: 241–250, 1978.

GRANTYN, R. AND GRANTYN, A. Morphological and electrophysiological properties of cat abducens motoneurons. *Exp. Brain. Res.* 31: 249–274, 1978.

HADIDIAN, Z. AND DUNN, M. S. Localization in the oculomotor nuclei of the goldfish. *J. Comp. Neurol.* 68: 191–203, 1938.

HENN, V. AND COHEN, B. Eye muscle motor neurons with different functional characteristics. *Brain Res.* 45: 561–568, 1972.

HENNEMAN, E., SOMJEN, G., AND CARPENTER, D. O. Functional significance of cell size in spinal motoneurons. *J. Neurophysiol.* 28: 560–580, 1965.

HERMANN, H. T. Eye movement correlated units in mesencephalic oculomotor complex of goldfish. *Brain Res.* 35: 240–244, 1971.

HORIKAWA, K. AND ARMSTRONG, W. E. A versatile means of intracellular labeling: injection of biocytin and its detection with avidin conjugates. *J. Neurosci. Methods* 25: 1–11, 1988.

IWAMOTO, Y., KITAMA, T., AND YOSHIDA, K. Vertical eye movement-related secondary vestibular neurons ascending in medial longitudinal fasciculus in cat. I. Firing properties and projection pathways. *J. Neurophysiol.* 63: 902–917, 1990.

KORN, H. AND BENNETT, M. V. L. Vestibular nystagmus and teleost oculomotor neurons: functions of electrotonic coupling and dendritic impulse initiation. *J. Neurophysiol.* 38: 430–451, 1975.

KUMARI, S., OJHA, J., SAHA, M. P., AND DATTA MUNSHI, J. S. Cytochemical differentiation of tonic (slow) and phasic (fast) muscle units in the ocular muscles of a fresh-water carp, *Catla catla* (Ham.). *Z. Mikrosk. Anat. Forsch. (Leipz.)* 93: 559–567, 1979.

LENNERSTRAND, G. AND BAKER, R. Motoneuronal innervation and mechanical properties of extraocular muscles in the catfish (*Ictalarus punctatus*). *Acta Physiol. Scand.* 131: 361–369, 1987.

LUITEN, P. G. M. AND DIJKSTRA-DE VLIEGER, H. P. Extraocular muscle representation in the brainstem of the carp. *J. Comp. Neurol.* 179: 669–676, 1978.

MESULAM, M.-M. Principles of horseradish peroxidase neurohistochemistry and their applications for tracing neural pathways—axonal transport, enzyme histochemistry and light microscopic analysis. In: *Tracing Neural Connections With Horseradish Peroxidase,* edited by M.-M. Mesulam. New York, 1982, p. 1–151.

MONTGOMERY, J. C. Eye movement dynamics in the dogfish. *J. Exp. Biol.* 105: 297–303, 1983.

MONTGOMERY, J. C. AND MACDONALD, J. A. Oculomotor function at low temperature: antarctic versus temperate fish. *J. Exp. Biol.* 117: 181–191, 1985.

MONTGOMERY, J. C. AND PAULIN, M. G. The effects of temperature on the characteristics of the dogfish oculomotor system. *J. Exp. Biol.* 113: 101–107, 1984.

OPTICAN, L. M. AND MILES, F. A. Visually induced adaptive changes in primate saccadic oculomotor control signals. *J. Neurophysiol.* 54: 940–958, 1985.

PASTOR, A. M. AND BAKER, R. Activity of medial rectus motoneurons in goldfish during vestibular and visual evoked eye movements. *Soc. Neurosci. Abstr.* 15: 807, 1989.

PASTOR, A. M., TORRES, B., AND DELGADO-GARCÍA, J. M. Behavior of medial rectus motoneurons in the alert goldfish. *Eur. Neurosci. Assoc. Abstr.* 13: 34, 1989.

ROBINSON, D. A. The mechanics of human saccadic eye movement. *J. Physiol. Lond.* 174: 245–264, 1964.

ROBINSON, D. A. Oculomotor unit behavior in the monkey. *J. Neurophysiol.* 33: 393–404, 1970.

SKAVENSKY, A. AND ROBINSON, D. A. Role of abducens neurons in vestibuloocular reflex. *J. Neurophysiol.* 36: 724–737, 1973.

STAHL, J. S. AND SIMPSON, J. I. Responses of abducens neurons to vestibular stimulation in awake rabbit. *Soc. Neurosci. Abstr.* 14: 955, 1988.

STEIN, R. B. AND BERTOLDI, R. The size principle: a synthesis of neurophysiological data. In: *Progress in Clinical Neurophysiology. Motor Unit Types. Recruitment and Plasticity in Health and Disease,* edited by J. E. Desmedt. Basel: Karger, 1981, vol. 9, p. 85–96.

STERLING, P. Anatomy and physiology of goldfish oculomotor system. I. Structure of abducens nucleus. *J. Neurophysiol.* 40: 557–572, 1977.

SZABO, T., LAZAR, G., LIBOUBAN, S., TOTH, P., AND RAVAILLE, M. Oculomotor system of the weakly electric fish *Gnatonemus petersii. J. Comp. Neurol.* 264: 480–493, 1987.

ULFHAKE, B. AND KELLERTH, J. O. Does α-motoneurone size correlate with motor unit type in cat triceps surae? *Brain Res.* 251: 201–209, 1982.